RSC Advances

ROYAL SOCIETY OF CHEMISTRY

www.rsc.org/advances

Synthesis and characterization of $Sr_{0.95}Y_{0.05}TiO_{3-\delta}$-based hydrogen electrode for reversible solid oxide cells

Yihan Ling[a,b]*, Luyang Chen[c], Bin Lin[d], Weili Yu[d], Tayirjan T. Isimjan[d], Ling Zhao[e]*, Xingqin Liu[a]

[a]CAS Key Laboratory of Materials for Energy Conversion, Department of Materials Science and Engineering, University of Science and Technology of China (USTC), Hefei, Anhui 230026, PR China

[b]Institute of Multidisciplinary Research for Advanced Materials, Tohoku University, Sendai 980-8577, Japan

[c]World Premier International (WPI) Research Center, Advanced Institute for Materials Research, Tohoku University, Sendai 980-8577, Japan

[d]Division of Physical Sciences and Engineering King Abdullah University of Science and Technology 4700 KAUST, Thuwal, 23955-6900 Saudi Arabia

[e]Department of Material Science and Chemistry, China University of Geoscience, Wuhan 430074, PR China

[*] Corresponding Author:

Yihan Ling*

Department of Materials Science and Engineering

University of Science and Technology of China

(USTC) Hefei, Anhui, 230026 P.R. China

(E-mail): lyhyy@mail.ustc.edu.cn

Abstract

Reversible solid oxide cells (RSOCs) can generate electricity as solid oxide fuel cells (SOFC) facing with a shortage of electricity, and can also store the electricity as solid oxide electrolysis cells (SOEC) at the time of excessive electricity. A composite $Sr_{0.95}Y_{0.05}TiO_{3-\delta}$-$Sm_{0.2}Ce_{0.8}O_{1.9}$ (SYT-SDC) as the hydrogen electrode provides a promising alternative for a conventional Ni/YSZ. The possible charge compensation mechanism of SYT is described as $Sr_{0.95}Y_{0.05}Ti^{4+}_{0.95-2\delta}Ti^{3+}_{2\delta+0.05}O_{3-\delta}$. The Ti^{3+} is approximately 11.73% in the reduced SYT by XRD Rietveld refinement, Electron Paramagnetic Resonance (EPR) and thermogravimetry (TG) analysis. Voltage-current curves and impedance spectra are measured as a function of applied voltages to characterize the cells. The bulk resistance (R_o) and the electrode polarization resistance (R_p) at open circuit voltages (OCV) at 750 °C are 9.06 Ωcm^2 and 10.57 Ωcm^2, respectively. The R_o values have a small amount of changes with small slopes both SOFC (-0.29 $\Omega cm^2\ V^{-1}$) and SOEC mode (0.5 $\Omega cm^2\ V^{-1}$), while the R_p values decrease all the time with the increasing voltages at both SOFC (-2.59 $\Omega cm^2\ V^{-1}$) and SOEC mode (-9.65 $\Omega cm^2\ V^{-1}$), indicating that the electrical conductivity and electro-catalytic property of SYT-based hydrogen electrode can be improved under the SOEC mode.

Keywords: Reversible solid oxide cells; Hydrogen electrode; Electron Paramagnetic Resonance; Electrode polarization resistance.

1. Introduction

Reversible solid oxide cells (RSOCs) have drawn more and more attention as a cost-effective energy regeneration and storage system due to its promising solution to the continuous supply of electrical energy, which could play a role of solid oxide fuel cells (SOFC) at the time of electricity shortage, and could also act as solid oxide electrolysis cells (SOEC) for use of excessive electricity.[1-4] Generally speaking, SOFC and SOEC modes essentially differ in the chemical potential gradient and electrical potential gradient, leading to the electrode materials with much higher requirements for meeting the performance and long-time stability of RSOCs.[5-6]

Ni/YSZ cermet, a conventional SOFC anode material, is directly used as a hydrogen electrode material for high-temperature steam electrolysis because of its excellent catalytic properties and suitable thermal expansion behavior. However, the pre-reduction of Ni/YSZ hydrogen electrode and a proper concentration of reducing gas are required to prevent the oxidization of metallic Ni metal which can increase the polarization resistance and even cause the failure for long-time testing.[7-10] Accordingly, Ni-based electrode may be inappropriate for RSOCs based on the above challenges, thus, it is necessary to find a nickel-free, more stable and highly active hydrogen electrode for RSOCs to obtain high performance and long-term stability. $(La_{0.75}Sr_{0.25})_xCr_{0.5}Mn_{0.5}O_3$ (LSCM) based materials have been widely reported to be electrochemically active and redox-stable SOFC anode materials, which can be potentially used as SOEC hydrogen electrode materials.[11-13] But under strong reducing potential conditions or high voltage applied to electrolysis, unfortunately, LSCM would be unstable with structural transformation.[14-15] The perovskites, $SrTiO_3$ with doping donors such as La^{3+} or Y^{3+} on the Sr^{2+} sites, are active and redox-stable materials that

have high n-type conductivity upon reduction with a highly attraction working as electrode materials.[16-25] Kim *et al.*[24] reported that the electrochemical reaction kinetic and the number of active electrochemical reaction sites of $Sr_{0.92}Y_{0.08}TiO_{3-\delta}$ anode by $Sm_{0.2}Ce_{0.8}O_{1.9}$ (SDC) coating were greatly improved. To the best of our knowledge, $Sr_{0.95}Y_{0.05}TiO_{3-\delta}$-$Sm_{0.2}Ce_{0.8}O_{1.9}$ (SYT-SDC) as the hydrogen electrode has not been reported to date. In this study, the oxidized and reduced SYT samples have been investigated by XRD Rietveld refinement, Electron Paramagnetic Resonance (EPR) and thermogravimetry (TG) analysis. Voltage-current curves and impedance spectra with the RSOCs configuration of (hydrogen electrode) SYT-SDC/YSZ/LSM-YSZ (air electrode) were measured as a function of applied voltages.

2. Experimental

2.1 Preparation of SYT, SDC, YSZ and LSM powders

The SYT powder was prepared through an EDTA–citrate complexation process. A suitable amount of EDTA was dissolved into distilled water with ammonia added to obtain a transparent solution. First, $Ti(OCH(CH_3)_2)_4$ was dissolved into nitrate solution, which then mixed nitrate solution of Sr^{2+} and Y^{3+} in the designed ratio and blended with the EDTA solution, and then added with citric acid as chelate to form a precursor solution. Molar ratio of metallic cations, EDTA and citric acid were set as 1:1.5:1.5. The precursor solution was stirred for 2 h and then heated on a hot plate at 100 °C to form a wet gel, which was then heated to form a dry gel at 200-300 °C and further burned into black sponge after evaporation. The fresh powders were calcined at 1000 °C for 2 h in air to form oxidized SYT. SDC, YSZ and LSM powders were prepared by auto-ignition process as described previously.[26]

2.2 Fabrication the RSOCs of SYT-SDC/YSZ/LSM-YSZ

The YSZ powder was dry-pressed into a green disk with a diameter of 16 mm followed by sintering in air at 1500 °C for 5 h to prepare 2-mm-thick YSZ electrolyte supports. Two surfaces of the electrolyte supports were mechanically polished and ultrasonically cleaned in ethanol and distilled water. SYT and SDC powders (at a ratio 60:40 by mass) were mixed thoroughly with a 6 wt.% ethylcellulose-terpineol binder to prepare the hydrogen electrode slurry, which was then painted on the YSZ electrolyte and sintered at 1150 °C for 3 h in air. Composite LSM-YSZ slurries were prepared by the same method, which was painted on the other side of YSZ electrolyte and sintered at 950 °C for 3 h in air. Silver paste was printed onto both electrode surfaces for current collecting.

2.3 Characterization

Amount of oxidized SYT powder was treated upon 100% H_2 at 1400 °C for 5 h to form the reduced SYT. The X-ray diffraction (XRD, θ= 1^o min^{-1}) was performed to analyze the phase purity of the oxidized and reduced SYT, then XRD Rietveld refinements were performed using GSAS software. The chemical compatibility of SYT-YSZ composite was investigated by mixing thoroughly SYT with YSZ in a 1:1 weight ratio, and then sintered at 1500 °C for 5 h in air as well as SYT with SDC. Electron Paramagnetic Resonance (EPR) of the reduced SYT powder was recorded at 150 K to confirm the presence of high spin Ti^{3+}. TG tests of the oxidized and reduced SYT samples were conducted on the thermal analyser at 10 ^{o} min^{-1} in air (TGA Q5000IR). Approximately 1.5 g of SYT powder was pressed into a bar and then sintered at 1450 °C for 10 h in 100% H_2, and the relative density reached 95%. The conductivity tests in reducing atmosphere were performed using a DC four-terminal

method from 50 °C to 750 °C in 100% H_2. The RSOCs were tested at 750 °C in a home-developed cell testing system with humidified hydrogen (3% H_2O) and air as a reactant, respectively.[27] The flow rate of hydrogen was 40 ml min^{-1}. The AC impedance spectra of single cells were measured under open circuit conditions and bias voltages using an electrochemical work station (IM6e, Zahner). The measurements were conducted in the range of 1 MHz–0.1 Hz with 10 mV amplitude.

3. Results and Discussion

3.1 Crystal structure

Fig. 1 shows the XRD Rietveld refinement results of the oxidized and reduced SYT powder, where the strong peaks correspond to space group Fm-3m (221) and no additional impurities are observed. The phase structure after 100% H_2 sintering at 1400 °C for 5 h was well maintained, which indicated SYT materials have an excellent stability under the strong reducing condition. The refinement of both oxidized and reduced SYT sample gave χ^2, wR_p and R_p values of 5.547, 9.91% and 6.64% as well as 9.532, 14.44% and 10.6%, respectively, indicating a close fit to experimental data. After reducing, the lattice parameter (a) of SYT decreased from 3.903371 Å to 3.901100 Å, which can be understood due to the two combined mechanisms of the formation of oxygen vacancies and charge compensation by partial reduction of Ti^{4+}. To further clarify the structure of the reduced SYT by the typical transmission electron microscope (TEM) image, Fig. 2(a) shows that the particle morphology of the reduced SYT particles was regular in shape and agglomerated, with an average particle size in the range 0.3-0.5 μm. The structural analysis from a HRTEM image as shown in Fig. 2(b) further reveals that the reduced SYT particles are high crystallinity and the interplanar

distance is clearly discerned to be 0.393 nm, corresponding to that of (100) plane, indicating that SYT sample calcined at high temperature strong reducing condition is still maintaining a cubic perovskite structure.

3.2 Electrical conductivity measurement

$SrTiO_3$ based materials as potential anode materials for SOFC are highly attractive because of their ideal thermal, chemical stability and semiconducting behavior. Fig. 3 shows the electrical conductivity of SYT sample sintered at 1450 ℃ for 10 h in 100% H_2 was measured in 100% H_2 in the temperature range of 50-750 ℃. The electrical conductivity increases with increasing temperature from room-temperature to 450 ℃, indicating a polaron type conduction mechanism. The SYT sample exhibited the maximum electrical conductivity of 58 S cm^{-1} at 450 ℃. At higher temperatures, the electrical conductivity decreases, suggesting that the electrical conduction of SYT transforms from the semi-conducting to the free electron and ion mixed conducting behavior (a metallic-type behavior), which is still much larger than that of $Sr_{0.92}Y_{0.08}TiO_3$ calcined and sintered both in air.[19] Generally, there are two possible ways under oxidation atmosphere that the introduction of Y^{3+} into Sr site of $SrTiO_3$ lattice. One way is that strontium vacancies will be formed by the formula.[19]

$$\frac{1}{2}Y_2O_3 \xrightarrow{SrTiO_3} Y_{Sr}^{\cdot} + \frac{1}{2}V_{Sr}^{''} + \frac{1}{2}SrO \quad (1)$$

The other is that the interstitial oxygen will be formed by the formula.[25]

$$\frac{1}{2}Y_2O_3 \xrightarrow{SrTiO_3} Y_{Sr}^{\cdot} + \frac{1}{2}O_i^{''} \quad (2)$$

While upon the reducing condition, Ti^{3+} ions can be formed by the electrovalent compensation

$$\frac{1}{2}Y_2O_3 \xrightarrow{SrTiO_3} Y_{Sr}^{\cdot} + Ti_{Ti}' \quad (3)$$

This suggests that the extra electrons at Ti sites can enter into the conduction band by the activation, leading to much higher electrical conductivity. Therefore, simple consideration of defect equilibrium in $Sr_{0.95}Y_{0.05}TiO_{3-\delta}$, the primary reaction of oxygen reduction can be represented as

$$2Ti_{Ti}^{\times} + O_O^{\times} \overset{K_{OX}}{\longleftrightarrow} 2Ti_{Ti}' + V_O^{\cdot\cdot} + \frac{1}{2}O_2(gas) \quad (4)$$

The equilibrium constant for reaction (1) can be presented as

$$K_{OX} = \frac{[Ti_{Ti}']^2[V_O^{\cdot\cdot}]P^{1/2}(O_2)}{[Ti_{Ti}^{\times}]^2[O_O^{\times}]} \quad (5)$$

The site conservation and charge neutrality requirement can be respectively expressed as

$$[Y_{Sr}^{\cdot}] = 0.05 \quad (6)$$

$$[Y_{Sr}^{\cdot}] + [Sr_{Sr}^{\times}] = 1 \quad (7)$$

$$[Ti_{Ti}'] + [Ti_{Ti}^{\times}] = 1 \quad (8)$$

$$[V_O^{\cdot\cdot}] + [O_O^{\times}] = 3 \quad (9)$$

$$[Ti_{Ti}'] = [Y_{Sr}^{\cdot}] + 2[V_O^{\cdot\cdot}] \quad (10)$$

The solid solution formula can be described as $Sr_{0.95}Y_{0.05}Ti^{4+}_{0.95-2\delta}Ti^{3+}_{2\delta+0.05}O_{3-\delta}$. Then, the equilibrium pressure of oxygen over $Sr_{0.95}Y_{0.05}TiO_{3-\delta}$ can be expressed as:

$$P^{1/2}(O_2) = \frac{K_{OX}(3-\delta)(0.95-2\delta)^2}{\delta(0.05+2\delta)^2} \quad (11)$$

Under a low oxygen partial pressure, much more oxygen vacancies and Ti^{3+} from the reduction of Ti^{4+} can happen. Electron-type carriers, Ti^{3+} (n=$[Ti_{Ti}']$), in $SrTiO_3$ with doping donors were reported earlier.[23, 28] Therefore, the electron concentration can be expressed as:

$$(\mathrm{n}-0.05)*\mathrm{n}^2 = 4\mathrm{K}_{\mathrm{OX}}(3-\delta)(0.95-2\delta)^2 * P^{-1/2}(\mathrm{O}_2) \quad (12)$$

Due to the very small value of δ, the equation (12) can be simplified to:$\mathrm{n} \propto P^{-1/6}(\mathrm{O}_2)$ dependence, which has a good agreement with literatures.[29-30] Electron concentration would increase with $P(\mathrm{O}_2)$ decreasing. Therefore, the experimental phenomenon is easy to understand that the electrical conductivity of reduced SYT sample is much larger than that of SYT.

3.3 Electron Paramagnetic Resonance(EPR) and thermogravimetry(TG) analysis

To further confirm the presence of Ti^{3+} in the reduced SYT sample, Electron Paramagnetic Resonance (EPR) was performed at 150 K to determine the presence of unpaired electrons of Ti^{3+} in the reduced SYT sample. As shown in Fig. 4(a), the reduced SYT sample showed a strong EPR signal at g = 1.958 characteristic of paramagnetic Ti^{3+} ions, directly proving the existence of Ti^{3+} species accompanied by the formation of oxygen vacancies.[31-33] In order to estimate the oxygen vacancy concentration of the reduced SYT sample, the weight changes measured by TG tests with the oxidized and reduced SYT samples were carried out in air as shown in Fig. 4(b). Supposing that the contents of variable oxygen vacancies of the oxidized SYT sample were almost filled by the environmental oxygen, then the oxygen vacancy concentration of reduced SYT sample can be approximately estimated. With the increasing temperatures, the oxidized SYT sample exhibited a series of weight losses, which mainly resulted from the lattice oxygen desorption with an oxygen desorption rate, while assumption of reaction (13) is a dynamic equilibrium with an oxygen absorption rate as follows:[34-35]

$$V_O^{\cdot\cdot} + 2Ti_{Ti}^{\prime} + \frac{1}{2}O_2(gas) \leftrightarrow O_O^{\times} \quad (13)$$

The higher the temperature, the shorter the relaxation time. As the temperature increases, the reduced SYT sample reached a maximum weight first at 1091 °C and then followed by a weight loss, which had the same trend with the literatures.[36] Since the reduced SYT sample was restored to form a large number of oxygen vacancies and Ti^{3+}species, with the increasing temperatures in air, the reduced SYT sample must absorb the environmental oxygen with an oxygen absorption rate, which must be higher than the oxygen desorption rate below 1091 °C. While the oxygen absorption rate was equal to the oxygen desorption rate around 1091 °C, the maximum weight for the reduced SYT sample was observed. Compared to the weight changes between oxidized and reduced SYT around this temperature, the variable oxygen vacancy concentrations of the reduced SYT sample was estimated to be 0.03365 because of the negligible weight change for Ti^{3+} species oxidation, and then the total concentration of Ti^{3+} species was calculated to be 0.1173. In this case, the reduced SYT can be described as $Sr_{0.95}Y_{0.05}Ti^{4+}_{0.8827}Ti^{3+}_{0.1173}O_{2.96635}$.

3.4 Electrochemical performances of RSOCs

Fig. 5 shows the voltage-current curves of RSOCs measured at 750 °C using 2-mm-thick YSZ as the electrolyte and SYT-SDC as the hydrogen electrode with humidified hydrogen (3% H_2O) as a reactant. The open circuit voltage (OCV) corresponding to zero current density was 0.9V, which could be influenced by the steam/hydrogen ratio and temperature.[37] The positive current density and the negative current density were observed with applied voltages to the SOFC mode and the SOEC mode, respectively. From the voltage-current curves, there is a smooth transition across OCV from the SOFC mode to the SOEC mode, indicating that the SYT-SDC/YSZ/LSM-YSZ cells are reversible for the charge transfer reaction. The

discharging and charging current densities were 18 mA cm^{-2} at 0.6 V and -23 mA cm^{-2} at 1.2 V, which showed a much better electrochemical performance under SOEC mode.

To further investigate the electrochemical process of RSOCs with SYT-SDC as hydrogen electrode at a variation of applied voltages, AC impedance spectroscopy was performed under the SOFC mode and the SOEC mode as shown in Fig. 6(a) and Fig. 6(b). In these spectra, the intercepts with the real axis at low frequencies represent the total cell resistance (R_t) of the cell and the value of the intercept at high frequency is bulk resistance (R_o) including the ohmic resistance of YSZ electrolyte, the ohmic resistance of porous electrodes and contact resistances of both electrodes, while the difference of the two values corresponds to the electrode polarization resistance (R_p) including the polarization losses of hydrogen electrode and air electrode. The R_o and R_p values with different applied voltages were measured at 750 °C shown in Fig. 7(a), for example at OCV, the R_o and R_p values are 9.06 Ωcm^2 and 10.57 Ωcm^2, respectively. The relationship between the resistance and the applied voltages (absolute values) can also be reflected from the results. It is observed that the *Ro* values had a small amount of changes with small slopes at both SOFC (-0.29 Ωcm^2V^{-1}) and SOEC mode (0.5 Ωcm^2V^{-1}) and a sudden decrease from SOFC mode to SOEC mode, while the R_p values decreased all the time with the increasing potentials both SOFC (-2.59 Ωcm^2V^{-1}) and SOEC mode (-9.65 Ωcm^2V^{-1}) and also had suddenly turning point at the OCV, which indicated that the electrode performance of SYT-SDC hydrogen electrode can be improved under higher applied voltages. For a better understanding the R_o and R_p value changes under the SOFC mode and the SOEC mode, the reaction zone of the mixed-conducting hydrogen electrodes can extend from the three phase boundary (TPB) to the gas/electrode interface through the chemical diffusion in the hydrogen electrode.

Because the difference of the electrochemical potential is the driving force for the electrode reaction, Fig. 8(a) shows the tendency of the local $P(O_2)$ changes of the hydrogen electrode under the SOFC mode and the SOEC mode. The local $P(O_2)$ can slightly increase under the SOFC mode and reduce under the SOEC mode.[38] According to the conductor mechanism of $SrTiO_3$-based materials,[29-30] the SYT-based hydrogen electrode can show better conductivity under SOEC mode than that under SOFC mode as shown in Fig. 8(b), indicating the electrical conductivity and electro-catalytic property can be improved.

To investigate the decreasing R_p values, two depressed arcs were observed for each impedance spectrum from Fig. 6, implying two rate-limiting steps, where R_H and R_L represent high and low frequency polarization resistances were shown in Fig. 7(b). The high-frequency arc was attributed to the polarization during charge-transfer process of electrode, while the low-frequency was due to the adsorption and desorption on the electrode surface and the diffusion of oxygen and hydrogen species.[39-40] The decrease of R_H values from SOFC to SOEC mode means much better charge-transfer process of electrode due to the increasing conductivity of SYT-SDC hydrogen electrode, while the decrease of R_L from SOFC to SOEC mode resulted from the improved LSM-YSZ oxygen electrode with an oxidizing atmosphere and electro-catalytic property of SYT-SDC hydrogen electrode for the steam electrolysis.

3.5 Stability test of RSOCs with SYT-SDC hydrogen electrode

Fig. 9(a) shows the chemical compatibility of SYT-YSZ composites were investigated by mixing thoroughly SYT with YSZ in a 1:1 weight ratio, and then sintered at 1500 °C for 5 h in air as well as SYT with SDC. There are no new peaks identifiable or shift of XRD peaks in the patterns indicating that there are no significant

reactions between SYT and others. Although interfacial reaction phenomenon between La-doped $SrTiO_3$ and $1CeO_2–10Sc_2O_3–89ZrO_2$ (ScSZ) electrolyte with $La_2Zr_2O_7$ impurity phase has been observed,[41] the short-term performance of RSOCs with SYT-SDC hydrogen electrode at 750 °C shows a stable electrochemical process as shown in Fig. 9(b), where the current density reached -23.6 $mAcm^{-2}$ with the applied electrical voltage of 1.2 V, indicating that SYT-SDC can be a potential hydrogen electrode for RSOCs.

3. Conclusion

In this work, $Sr_{0.95}Y_{0.05}TiO_{3-\delta}$ (SYT) was synthesized and characterized as the hydrogen electrode of oxygen-ion conducting RSOCs. XRD Rietveld refinement, Electron Paramagnetic Resonance and TG together demonstrated that the solid solution formula of the reduced SYT can be described as $Sr_{0.95}Y_{0.05}Ti^{4+}_{0.8827}Ti^{3+}_{0.1173}O_{2.96635}$. The reduced SYT was a typical n-type conductor with a total conductivity of 58 S cm^{-1} at 450°C. RSOCs with the cell configuration of SYT-SDC/YSZ/LSM-YSZ were assembled and evaluated. The electrical conductivity and the electro-catalytic property of The SYT-based hydrogen electrode could be improved under the SOFC mode. A stable steam electrolysis process was indicated by the short-term cell performance, where the current density reached 23.6 mA cm^{-2} at the applied voltage of 1.2 V at 750°C, indicating that SYT-SDC is a potential hydrogen electrode.

Acknowledgements

The authors wish to thank Japan Society for the Promotion of Science (JSPS) for

financial support through a Post-doctoral Fellowship for Foreign Researchers, and the financial support from Chinese Natural Science Foundation on contract No. 51102107.

Notes and references

1 M.A. Laguna-Bercero, *J. Power Sources*, 2012, **203**, 4.

2 M. Ni, *Int. J. Hydrogen Energ*. 2009, **34**, 7795.

3 A. Hauch, S.D. Ebbesen, S.H. Jensen and M. Mogensen, *J.Mat.Chem.*, 2008, **18**, 2331.

4 F. He, D. Song, R.R. Peng, G.Y. Meng and S. F. Yang, *J. Power Sources*, 2010, **195**, 3359.

5 K.F. Chen and S.P. Jiang, *Int. J. Hydrogen Energ*., 2011, **36**, 10541.

6 M. Keane, M.K. Mahapatra, A.Verma and P. Singh, *Int. J. Hydrogen Energ.*, 2012, **37**, 16776.

7 A. Hauch, S.H. Jensen, J.B. Bilde-Sørensen and M. Mogensen, *J. Electrochem. Soc.*, 2007, **154**, A619.

8 A. Hauch, S.D. Ebbesen, S.H. Jensen and M. Mogensen, *J. Electrochem. Soc*. 2008, **155**, B1184.

9 L. Holzer, B. Iwanschitz, T. Hocker, B. Münch, M. Prestat, D. Wiedenmann, U. Vogt, P. Holtappels, J. Sfeir, A. Mai and T. Graule, *J. Power Sources,* 2011, **196**, 1279.

10 J. Sehested, J.A.P. Gelten, I.N. Remediakis, H. Bengaard and J.K. Nørskov, *J. Catalysis,* 2004, **223**, 432.

11 X. Yang and J.T.S. Irvine, *J. Mat. Chem.,* 2008, **18**, 2349.

12 S.W. Tao, J.T.S. Irvine and J.A. Kilner, *Adv. Mater.,* 2005, **17**, 1734.

13 S.P. Jiang, L. Zhang and Y.J. Zhang, *J. Mater. Chem*., 2007, **17**, 2627.

14 G. Kim, G. Corre, J.T.S. Irvine, J.M. Vohs and R.J. Gorte, *Electrochem. Solid-State Lett.,* 2008, **11**, B16.

15 S.S. Xu, S.S. Li, W.T. Yao, D.H. Dong and K. Xie, *J. Power Sources,* 2013, **230**, 115.

16 D. Neagu and J.T.S. Irvine, *Chem. Mater.,* 2010, **22**, 5042.

17 J. Canales-Vazquez, M.J. Smith, J.T.S. Irvine and W.Z. Zhou, *Adv. Funct. Mater.,* 2005, **15**, 1000.

18 S.Li, Y.X. Li, Y. Gan, K.Xie and G.Y. Meng, *J. Power Sources*, 2012, **218**, 244.

19 X. Huang and H. Zhao, *J. Phys. Chem. Solids*, 2006, **67**, 2609.

20 S. Koutcheiko, Y. Yoo, A. Petric and I. Davidson, *Ceramics Internationa*l, 2006, **32**, 67

21 Y. Li, J. Zhou, D. Dong, Y. Wang, J.Z. Jiang, H. Xiang and K. Xie, *Phys. Chem. Chem. Phys.*, 2012, **14**, 15547.

22 O. A. Marina, N.L. Canfield and J. W. Stevenson, *Solid State Ionics*, 2002, **149**, 21

23 D. Burnat, A. Heel, L. Holzer, D. Kata, J. Lis and T. Graule, *J. Power Sources*, 2012, **201**, 26

24 H.S. Kim, S.P. Yoon, J.W. Yun, S.A. Song, S.C. Jang, S.W. Nam, Y.G. Shul, *Int. J.Hydrogen Energy*., 2012, **37**, 16130.

25 Q.L. Ma, F. Tietz, D. Stover, *Solid State Ionics*, 2011, **192**, 535

26 Y.H. Ling, J. Chen, Z.B. Wang, C.R. Xia, R.R. Peng and Y.L. Lu, *Int. J.Hydrogen Energy*., 2013, **38**, 7430.

27L. Zhao, B.B. He, Y.H. Ling, Z.Q. Xun, R.R. Peng, G. Y. Meng and X.Q. Liu, *Int. J. Hydrogen Energ*., 2010, **35**, 3769.

28 X. Li, H.L. Zhao, W. Shen, F. Gao, X.L. Huang, Y. Li and Z.M. Zhu, *J. Power Sources*, 2007, **166**, 47.

29 D.J. Cumming,V. V. Kharton, A. A. Yaremchenko, A. V. Kovalevsky and J. A. Kilner, *J. Am. Ceram.Soc.,* 2011, **94(9)**,2993.

30 E. Niwa, K. Sato, K.Yashiro, J. Mizusaki. *ECS Transactions*, 2009, **25 (2)**, 2631

31 S.V. Chong,J. Xia, N. Suresh, K. Yamaki and K. Kadowaki, *Solid State Commun.,* 2008, **148**, 345.

32 J. Soria, J. Sanz, I.Sobrados, J.M. Coronado, F. Fresno and M.D. Hernández-Alonso, *Catal. Today*, 2007, **129**, 240.

33 M.D. Glinchuk, I.P. Bykov, A.M. Slipenyuk, V.V. Laguta and L. Jastrabik, *Phy. Solid State*, 2001, **43**, 841.

34 L.W. Tai, M.M. Nasrallah and H.U. Anderson, *Solid State Ionics*, 1995, **76**, 259.

35 Y.H. Ling, L. Zhao, B. Lin, Y.C. Dong, X.Z. Zhang, G.Y. Meng and X.Q. Liu, *Int. J. Hydrogen Energ.,* 2010, **35**, 6905.

36 X. Li, H.L. Zhao, F. Gao, Z.M. Zhu, N. Chen and W. Shen, *Solid State Ionics*, 2008, **179**,1588.

37 C. Jin, C.H. Yang, F. Zhao, D. Cui and F.L. Chen, *Int. J. Hydrogen Energ.*, 2011, **36**, 6905.

38 T. Kawada, T. Watanabe, A. Kaimai, K. Kawamura, Y. Nigara, J. Mizusaki, *Solid State Ionics*, 1998, **108**, 391.

39 S. Li, Z. Lu, X. Huang, B. Wei and W. Su, *J. Phys. Chem. Solids*, 2007, **68**, 1707.

40 Y.H. Ling, X.Z. Zhang, S.W. Wang, L. Zhao, B. Lin and X.Q. Liu, *J. Power Sources,* 2010, **295**, 7042.

41 G. Chen, H. Kishimoto, K. Yamaji, K. Kuramoto and T. Horita, *J. Power Sources,* 2014, **246**, 49.

Figure Captions

Fig. 1 XRD Rietveld refinement of (a) $Sr_{0.95}Y_{0.05}TiO_{3-\delta}$ prepared by an EDTA–citrate complexation process calcined at 1000 °C for 2 h in air and (b) reduced in 100% H_2 at 1400 °C -5h.

Fig.2 (a) TEM image and (b) HRTEM image of the reduced $Sr_{0.95}Y_{0.05}TiO_{3-\delta}$ particles

Fig. 3 The electrical conductivity of the reduced $Sr_{0.95}Y_{0.05}TiO_{3-\delta}$ sample in 100% H_2 in the temperature range of 50 to 750 °C.

Fig. 4(a) Electron paramagnetic resonance (EPR) of reduced $Sr_{0.95}Y_{0.05}TiO_{3-\delta}$ powder conducted at the temperature of 150 K. (b) TG tests of oxidized and reduced $Sr_{0.95}Y_{0.05}TiO_{3-\delta}$ in air at 1200 °C at the rate of 10°C min^{-1}.

Fig. 5 Voltage-current density curves of RSOCs measured at 750 °C using 2-mm-thick YSZ as the electrolyte and SYT-SDC as the hydrogen electrode with humidified hydrogen (3% H_2O) as a reactant.

Fig. 6 In situ AC impedance of RSOCs at 750 °C with external applied voltages (a) under SOFC mode and (b) under SOEC mode

Fig. 7(a)The total cell resistance (Rt), bulk resistance(Ro), the electrode polarization resistance (Rp) and (b) high and low frequency polarization resistances (R_H and R_L) at 750 °C with the different applied voltages.

Fig. 8 (a) Schematic of the local $P(O_2)$ change of SYT-SDC hydrogen electrode and (b) the variation of electrical conductivity in $SrTiO_3$-based materials depend on the local $P(O_2)$ under SOFC mode and under SOEC mode

Fig. 9(a) Chemical compatibility of SYT-YSZ and SYT-SDC composites after sintered at 1500 °C for 5 h, respectively. (b) The short-term performance of RSOCs with SYT-SDC hydrogen electrode with an applied electrical voltage of 1.2 V at 750°C,

Figure 1

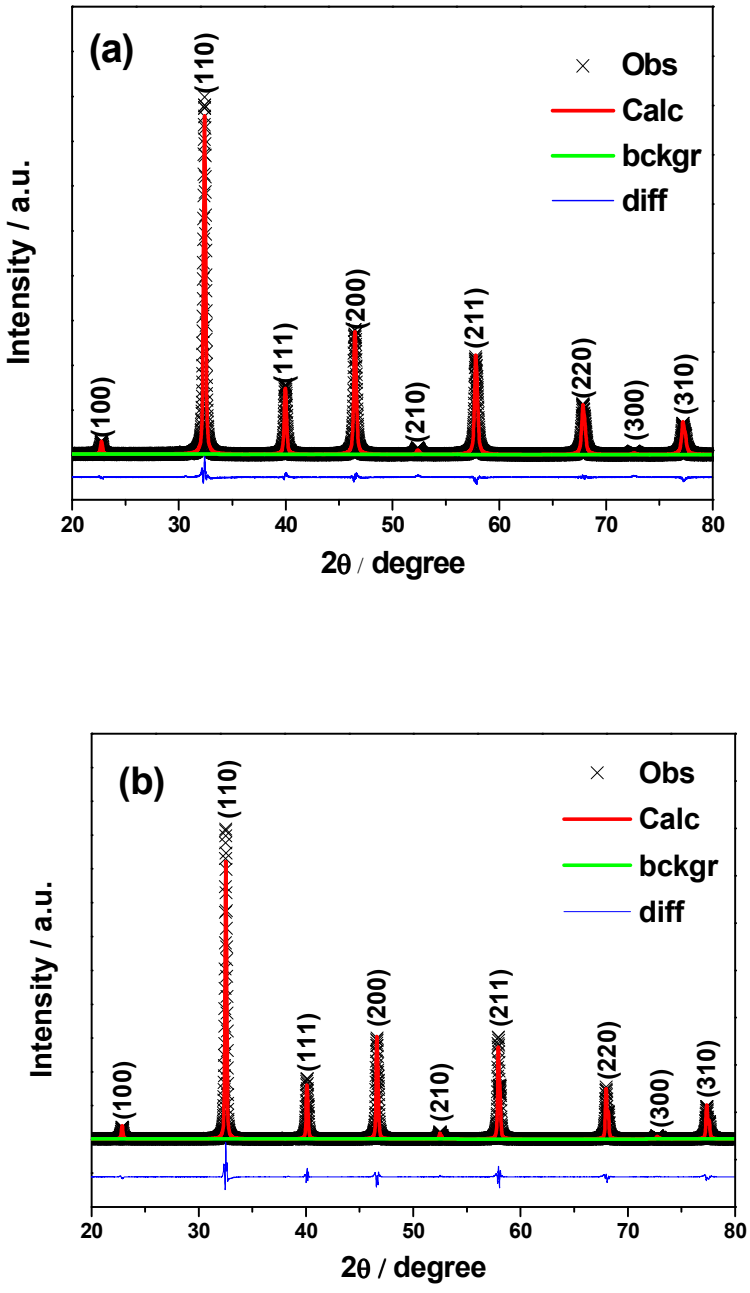

Figure 2

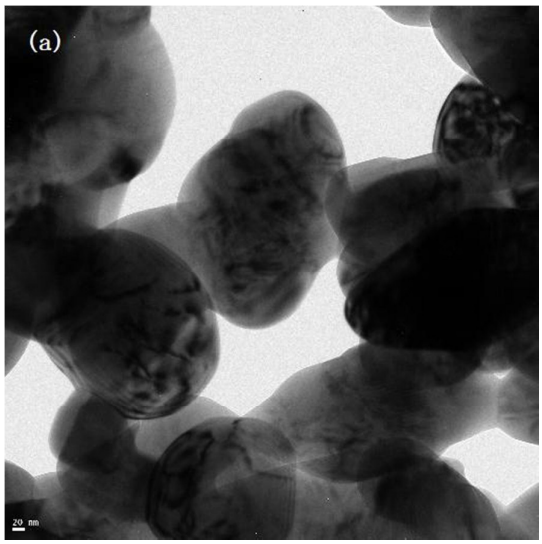

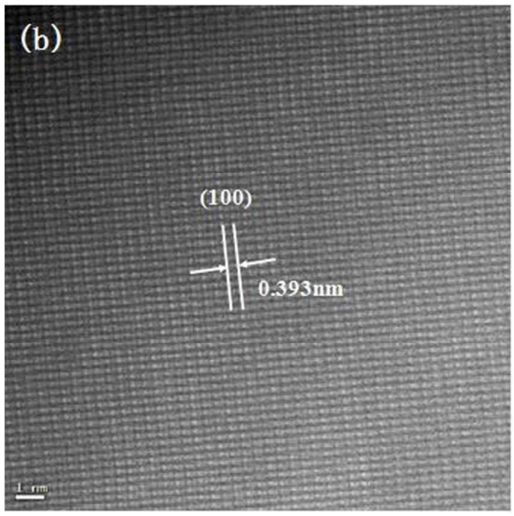

Figure 3

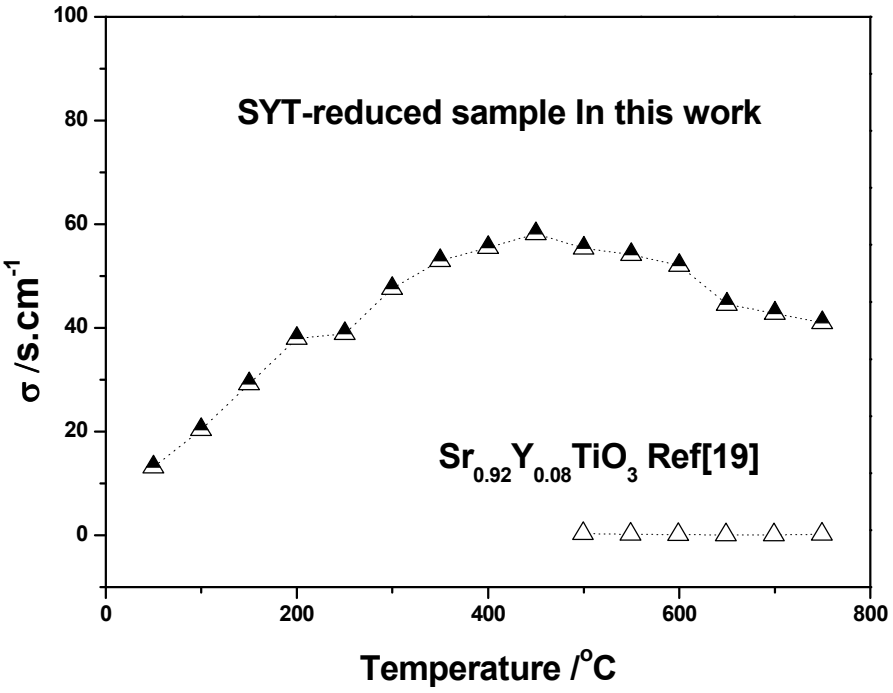

Figure 4

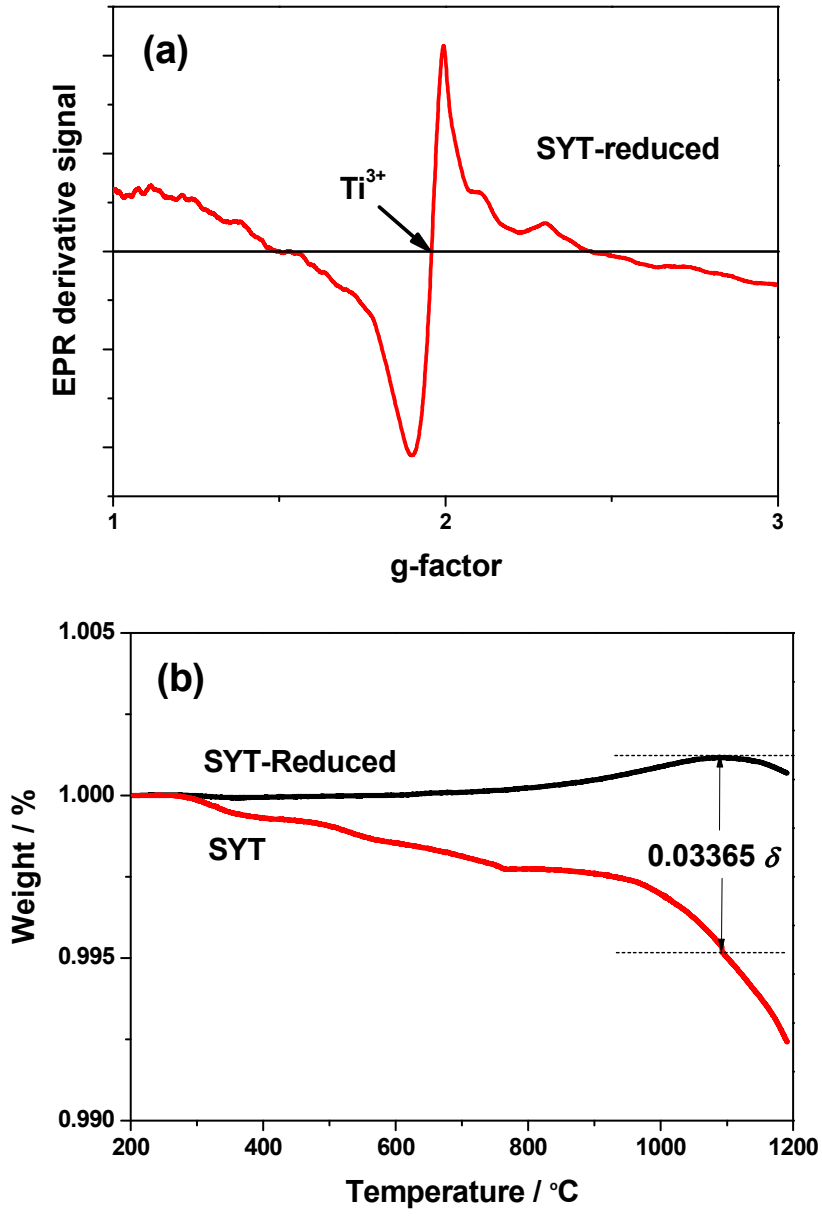

Figure 5

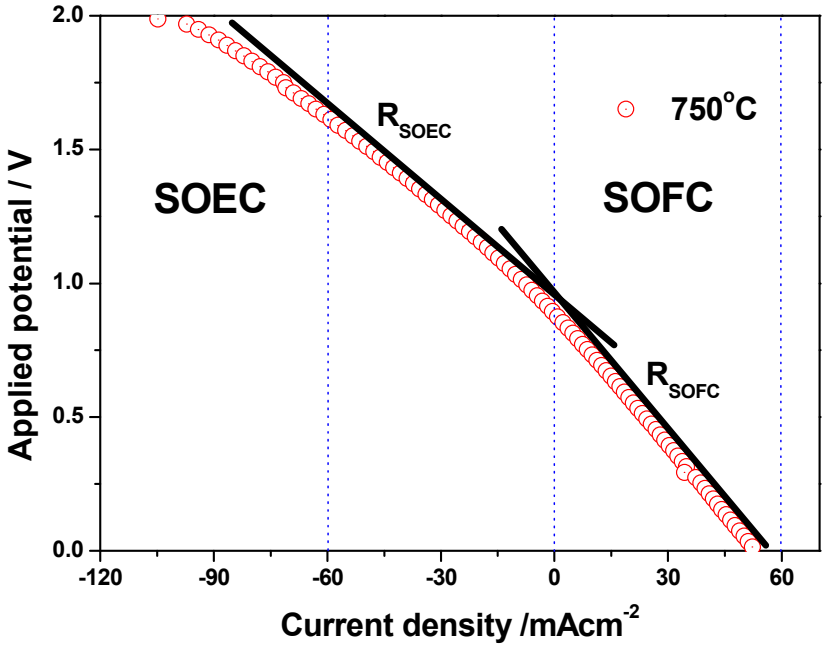

Figure 6

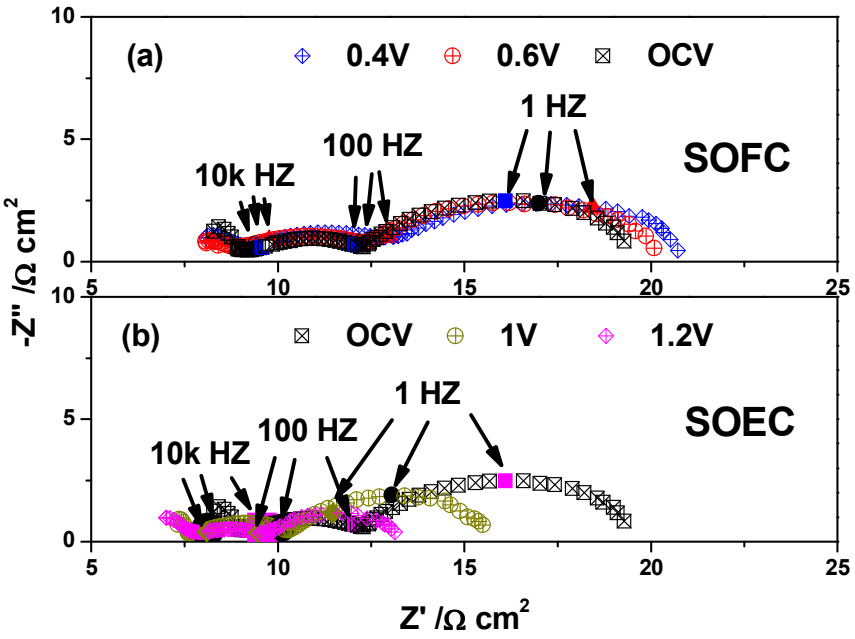

Figure 7

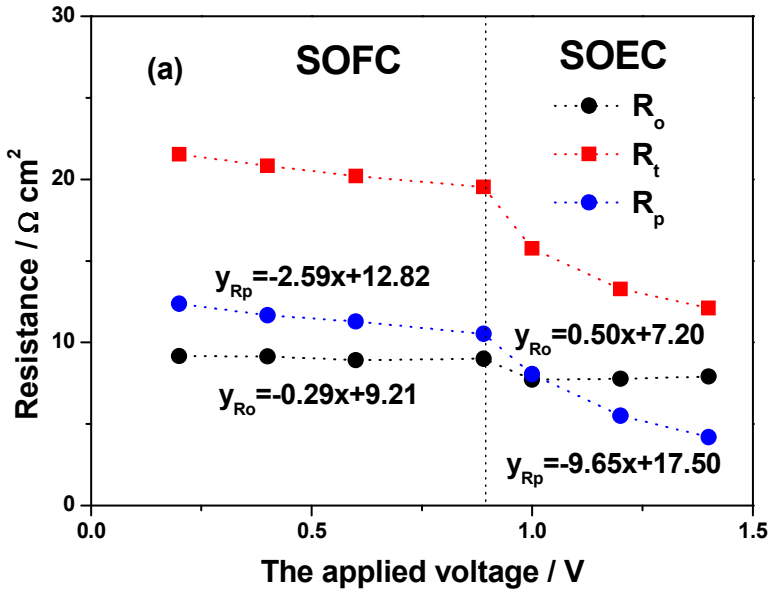

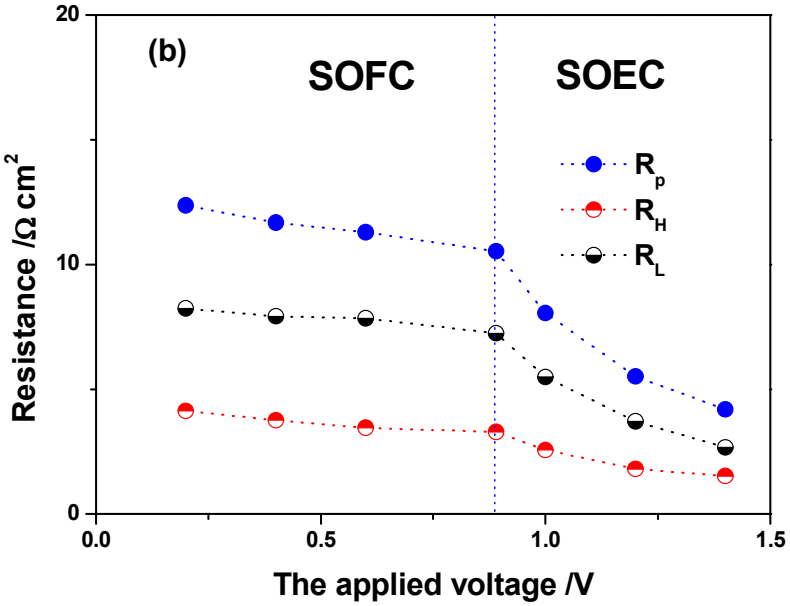

Figure 8

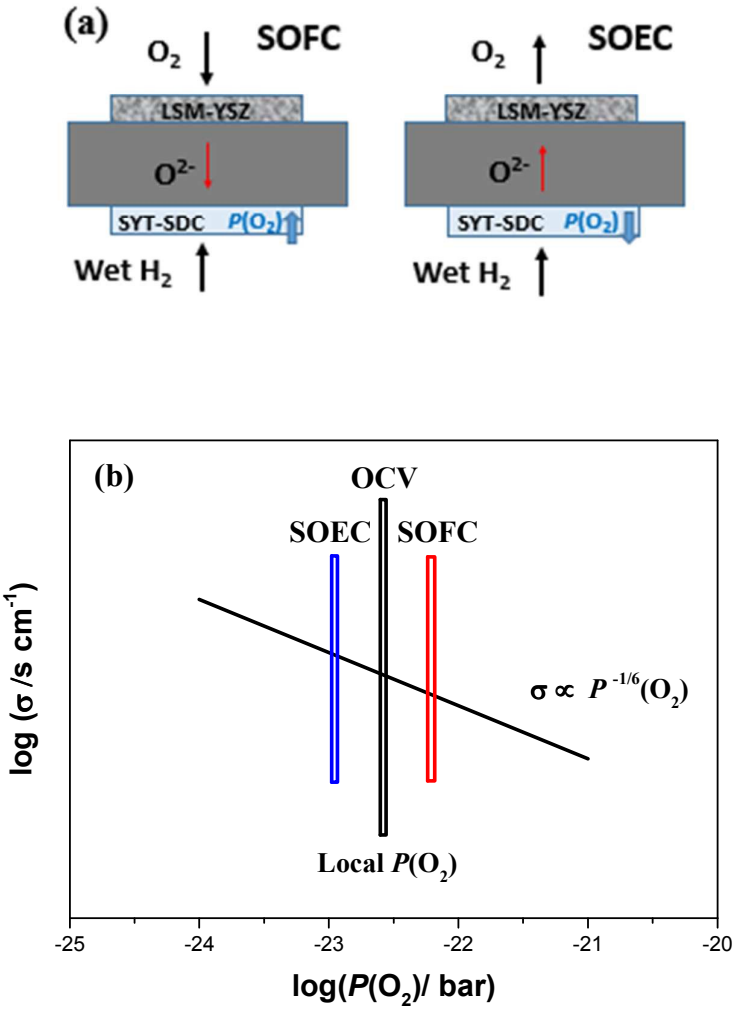

Figure 9